

Supporting information

One-dimensional lanthanide coordination polymers: syntheses, structures, and single-ion magnet property

Hung-Kai Feng, Po-Jung Huang and Hui-Lien Tsai*

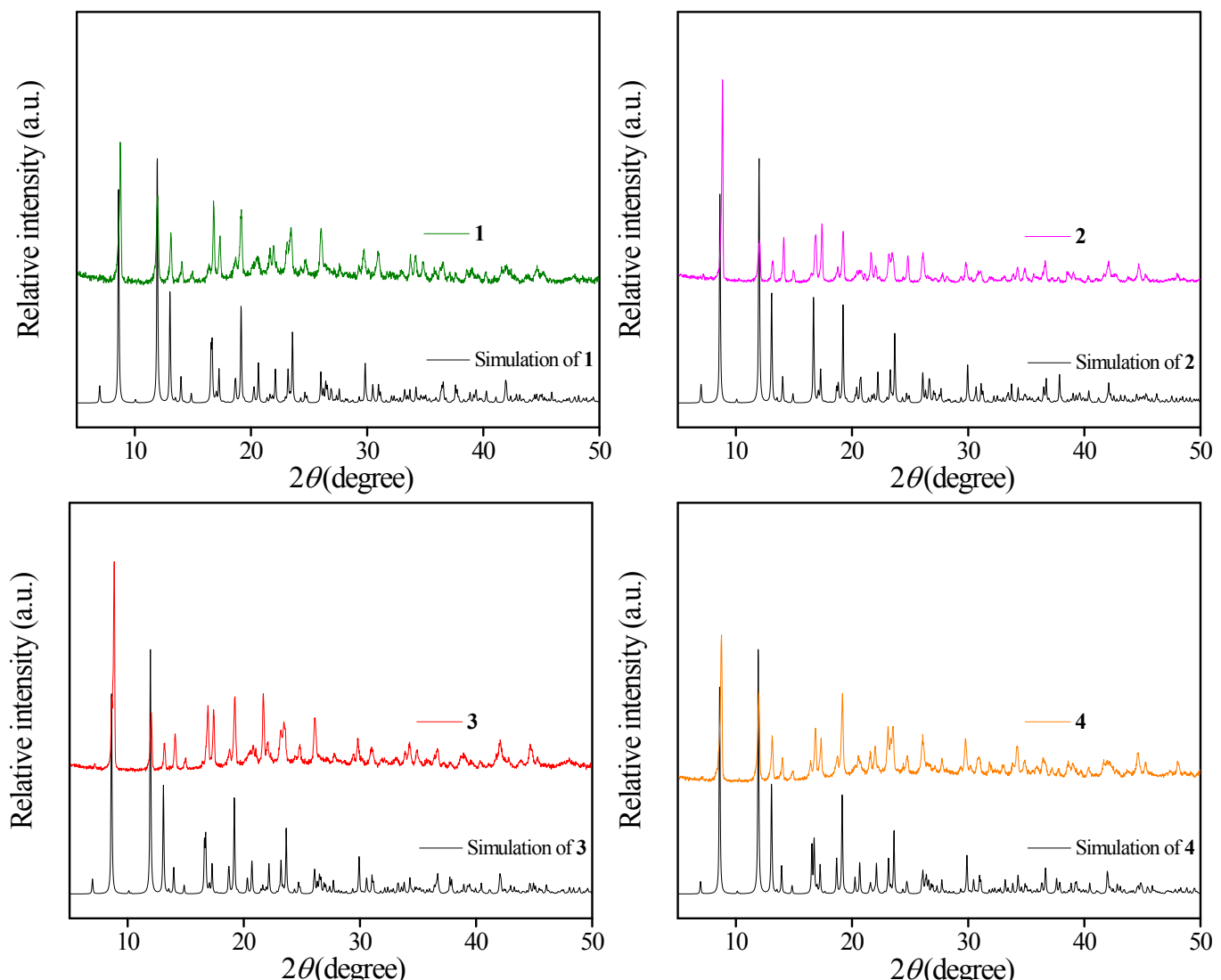


Fig. S1 Stimulated and experimental powder XRD patterns of complexes **1**, **2**, **3**, and **4**.

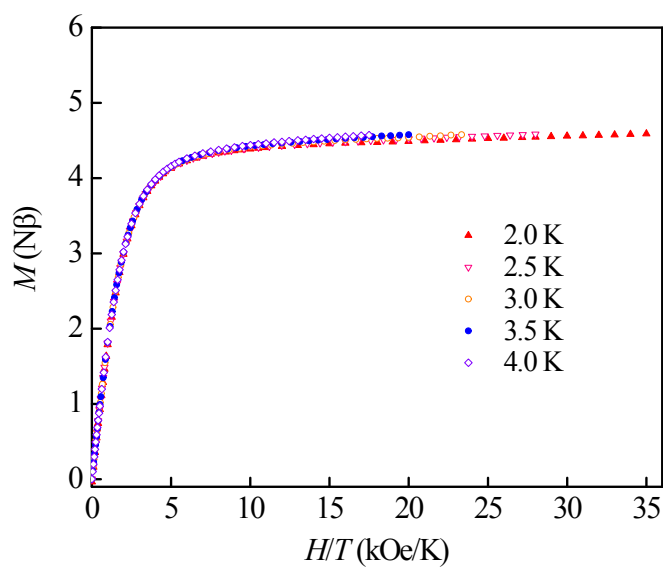


Fig. S2 Plots of reduced magnetisation M vs. H/T for complex **2** at 0–70 kOe and 2.0–4.0 K.

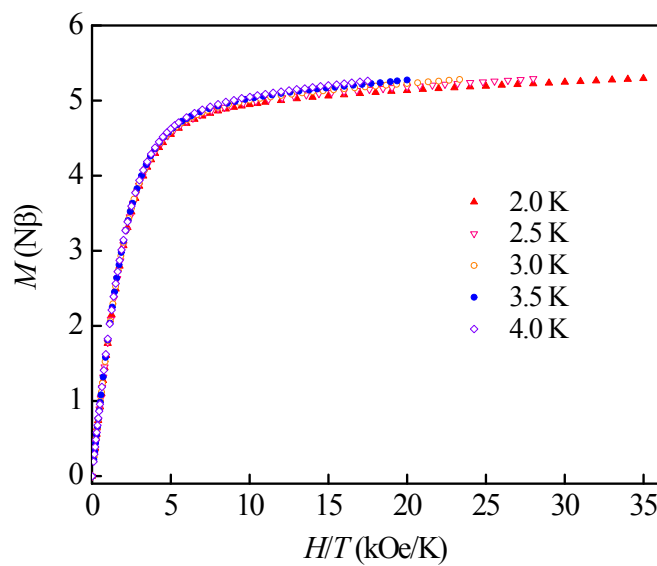


Fig. S3 Plots of the reduced magnetisation M vs. H/T for complex **1** at 0–70 kOe and 2.0–4.0 K.

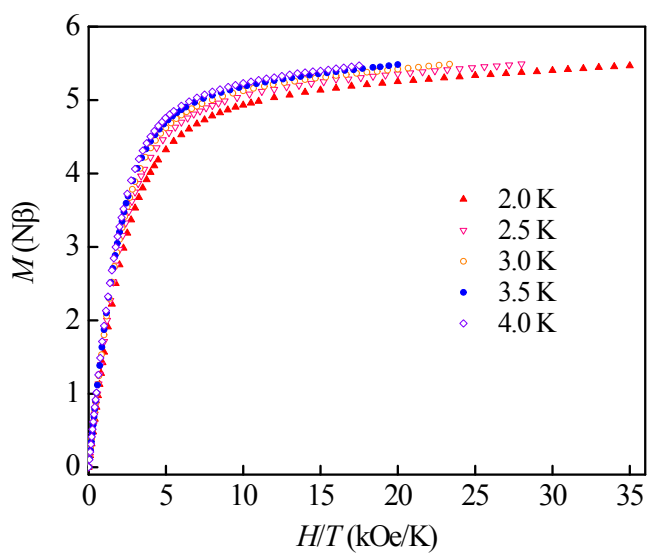


Fig. S4 Plots of the reduced magnetisation M vs. H/T for complex **3** at 0–70 kOe and 2.0–4.0 K.

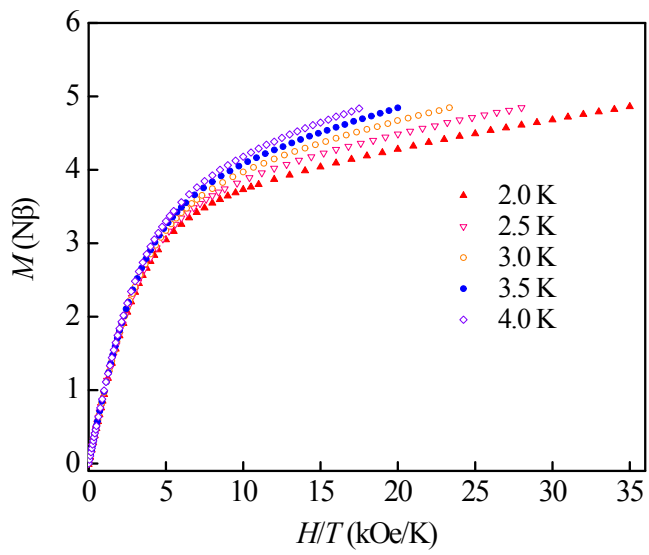


Fig. S5 Plots of the reduced magnetisation M vs. H/T for complex **4** at 0–70 kOe and 2.0–4.0 K.

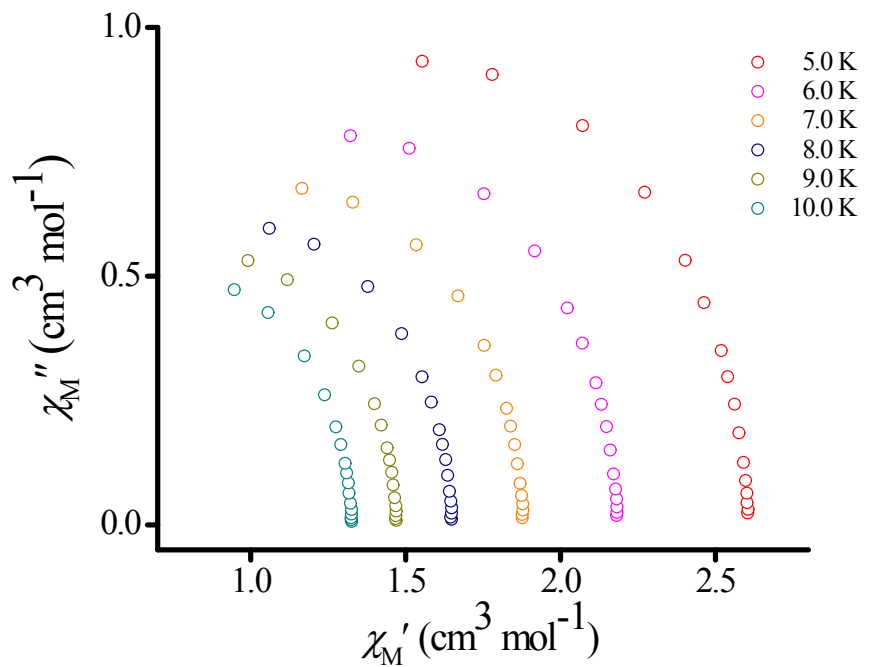


Fig. S6 Cole-Cole diagrams plotted in χ_M'' versus χ_M' for complex **2** in $H_{dc} = 0$.

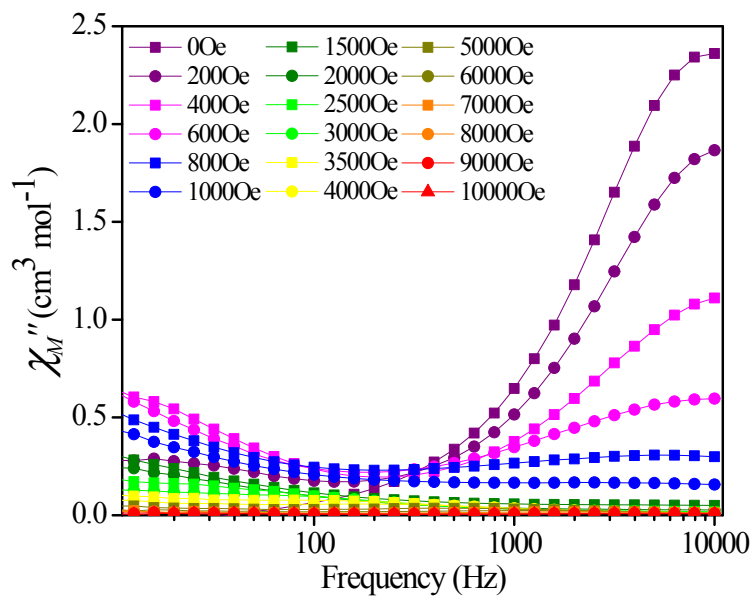


Fig. S7 Frequency dependence of the ac susceptibility measured in various external dc fields below 10000 Oe for complex **2** at 1.8 K.

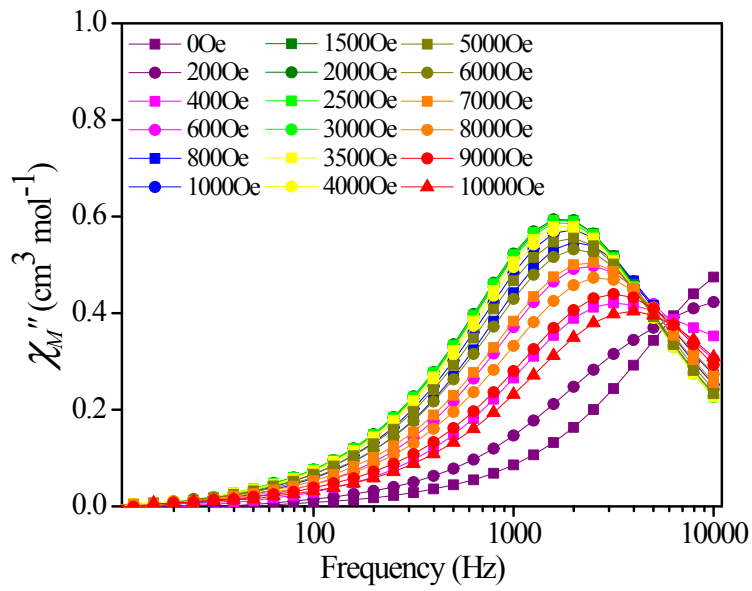


Fig. S8 Frequency dependence of the ac susceptibility measured in various external dc fields below 10000 Oe for complex **2** at 10 K.

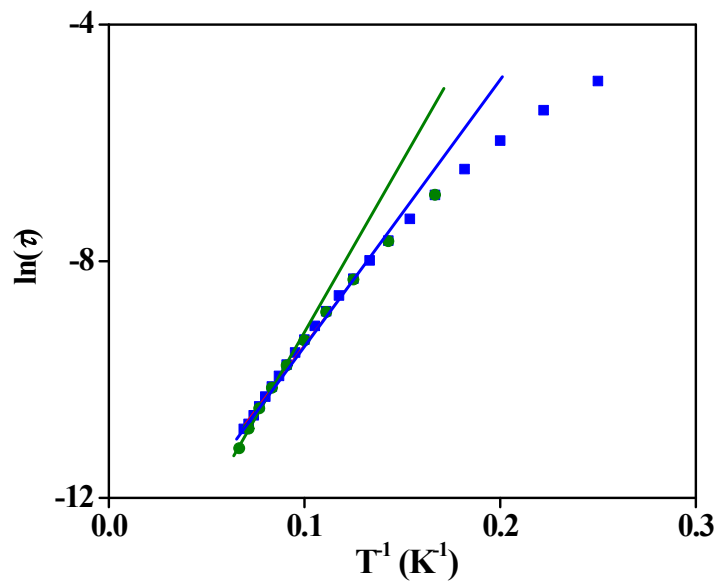


Fig. S9 $\ln(\tau)$ vs. T^{-1} plot for complex **2** obtained from (blue dots) frequency-dependent ac magnetic susceptibilities and the (green dots) Cole-Cole analyses under 3000 Oe dc field. The solid lines are the best fits.

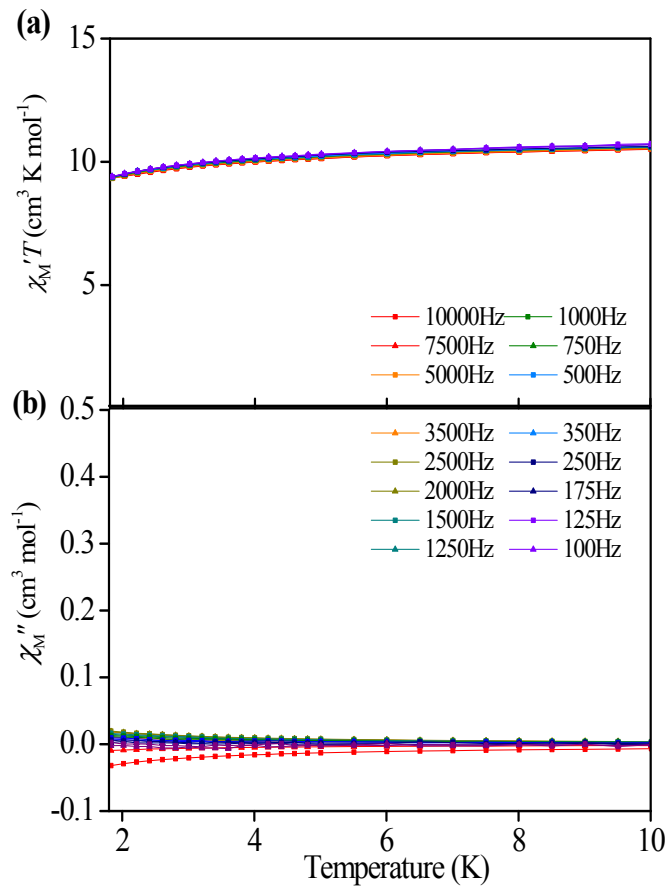


Fig. S10 (a) Plots of $\chi_M' T$ and (b) χ_M'' vs. temperature for a microcrystalline sample of complex **1** in a 3.5-Oe ac field and zero-dc field. The data were collected in an ac field oscillating at the indicated frequency.

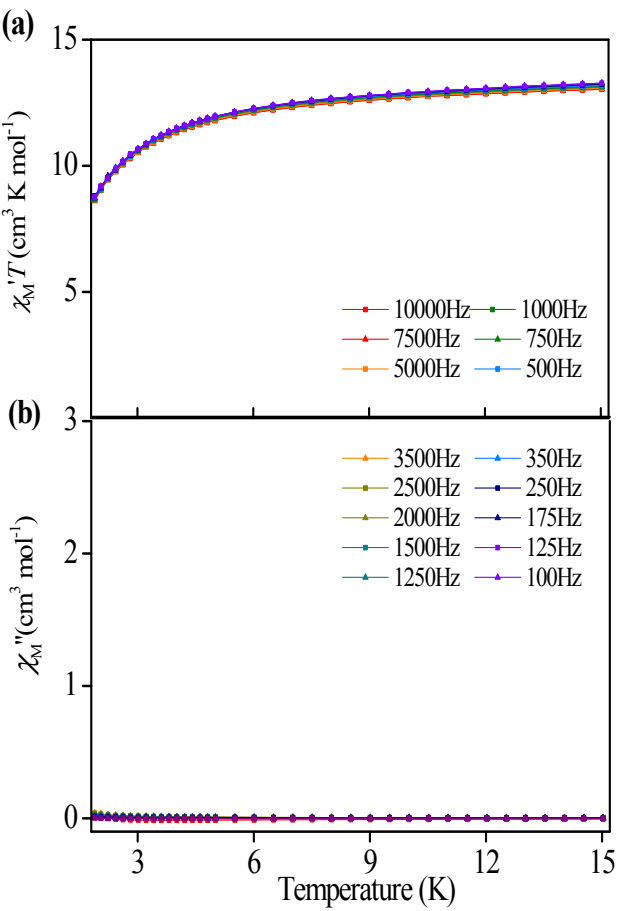


Fig. S11 (a) Plots of $\chi_M' T$ and (b) χ_M'' vs. temperature for a microcrystalline sample of complex 3 in a 3.5-Oe ac field and zero-dc field. The data were collected in an ac field oscillating at the indicated frequency.

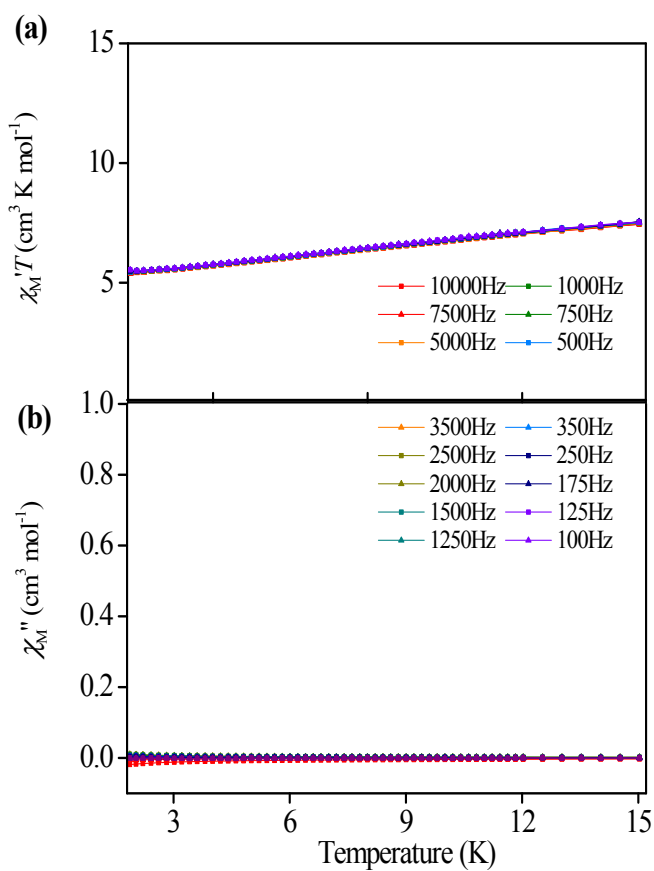


Fig. S12 (a) Plots of $\chi_M' T$ and (b) χ_M'' vs. temperature for a microcrystalline sample of complex 4 in a 3.5-Oe ac field and zero-dc field. The data were collected in an ac field oscillating at the indicated frequency.

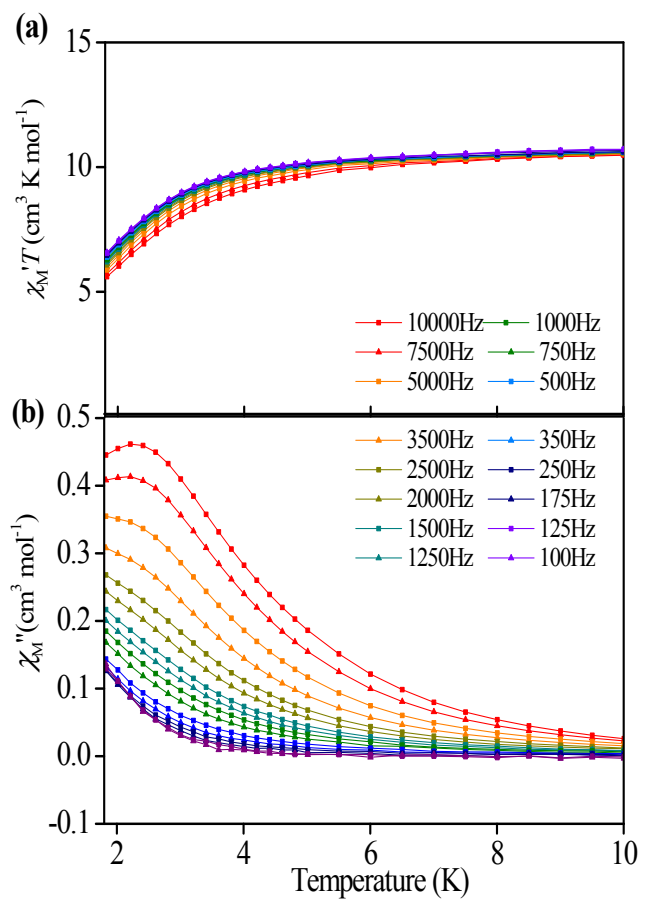


Fig. S13 (a) Plots of $\chi_M' T$ and (b) χ_M'' vs. temperature for a microcrystalline sample of complex **1** in a 1000 Oe dc field. The data were collected in an ac field oscillating at the indicated frequency.

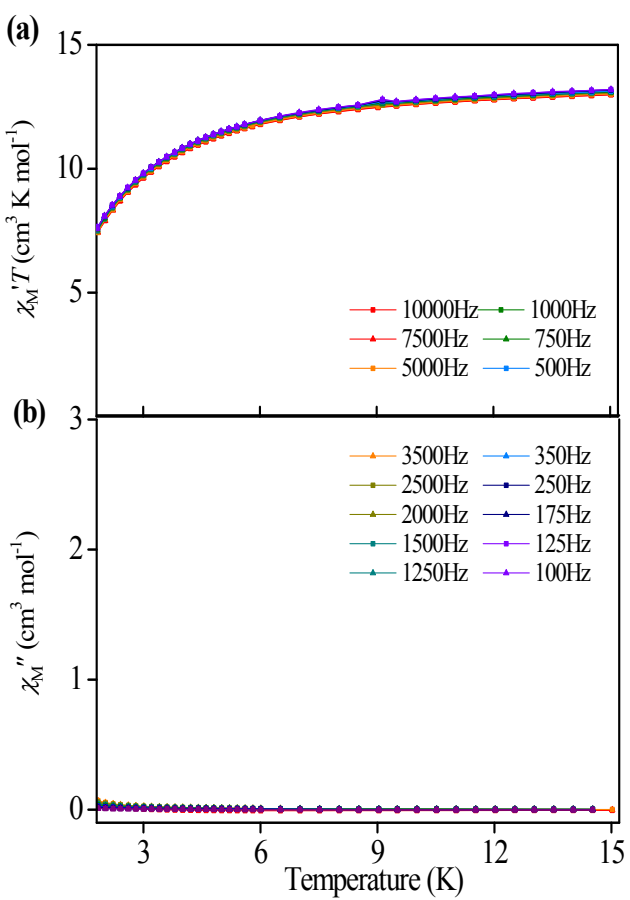


Fig. S14 (a) Plots of $\chi_M' T$ and (b) χ_M'' vs. temperature for a microcrystalline sample of complex 3 in a 1500 Oe dc field. The data were collected in an ac field oscillating at the indicated frequency.

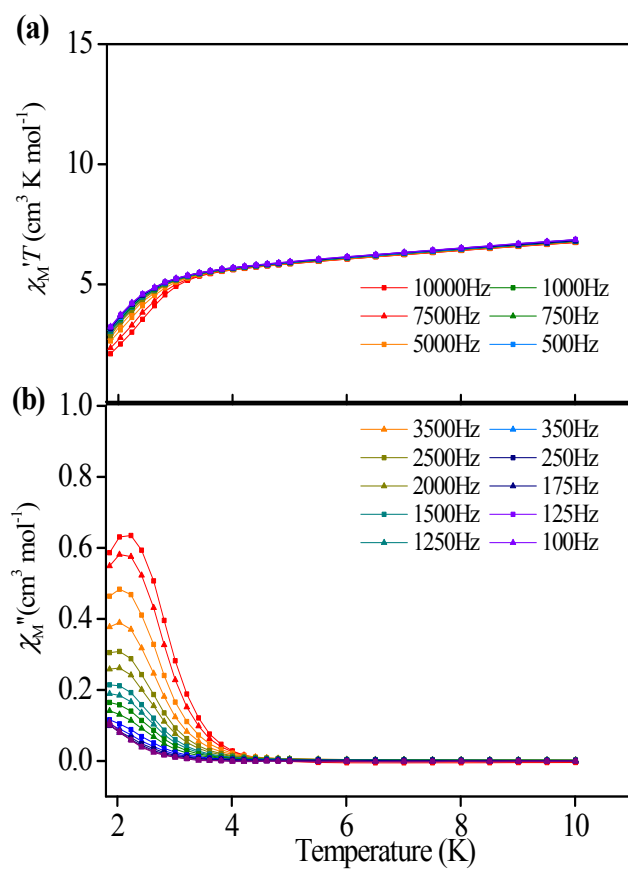


Fig. S15 (a) Plots of $\chi_M' T$ and (b) χ_M'' vs. temperature for a microcrystalline sample of complex 4 in a 1000 Oe dc field. The data were collected in an ac field oscillating at the indicated frequency.

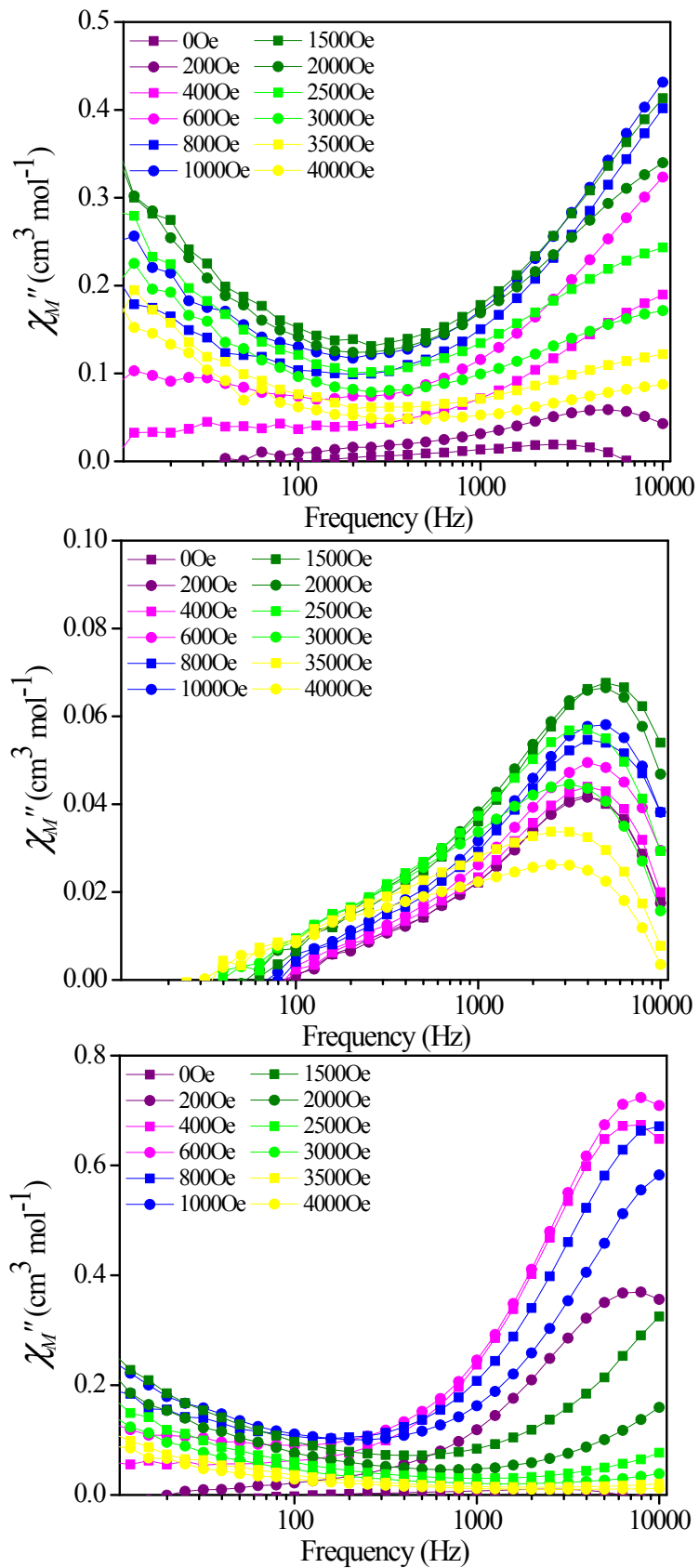


Fig. S16 Frequency dependence of the ac susceptibility measured in various external dc fields at 1.8 K for (top) **1**, (middle) **3**, and (bottom) **4**.

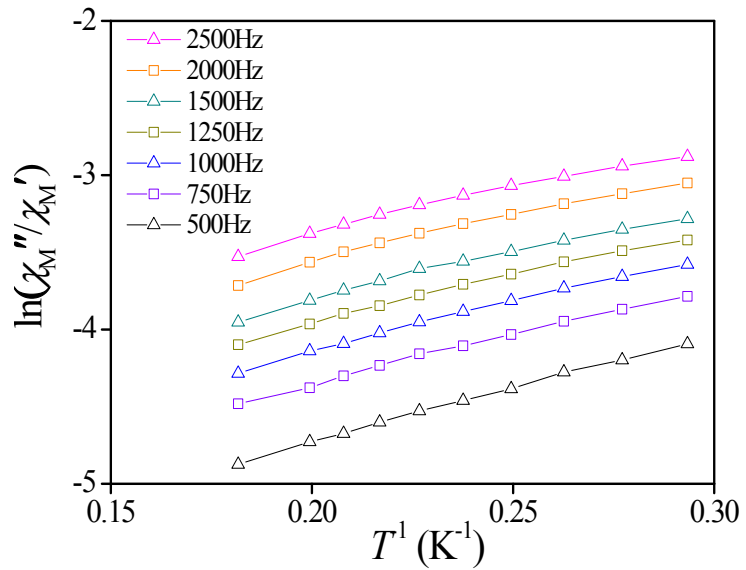


Fig. S17 Plot of natural logarithm of χ_M''/χ_M' vs. T^{-1} for **1**. The solid line represents the fitting results over the range 500–2500 Hz.

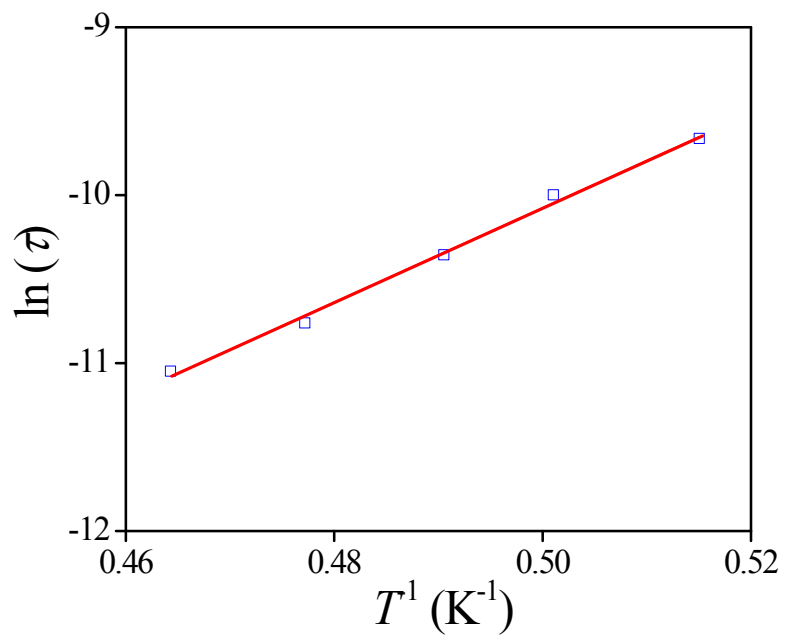


Fig. S18 Relaxation time of magnetisation $\ln(\tau)$ vs. T^{-1} plot for complex **4** obtained from frequency-dependent ac magnetic susceptibility measurements under 1000 Oe dc field. Solid line was fitted with the Arrhenius law.

Table S1 Selected bond distances (\AA) and bond angles ($^\circ$) for complexes **1**, **2**, **3**, and **4**.

Complex 1			
Tb(1)-O(1)	2.188(3)	Tb(1)-O(2)	2.372(2)
Tb(1)-O(3)	2.241(2)	Tb(1)-O(6)	2.497(2)
Tb(1)-O(4)	2.332(3)	Tb(1)-O(7)	2.492(3)
Tb(1)-O(5)	2.355(3)	Tb(1)-N(1)	2.559(3)
O(1)-Tb(1)-O(3)	94.18(10)	O(2)-Tb(1)-O(7)	138.67(9)
O(1)-Tb(1)-O(4)	150.74(10)	O(1)-Tb(1)-O(6)	77.01(9)
O(3)-Tb(1)-O(4)	90.53(12)	O(3)-Tb(1)-O(6)	75.59(8)
O(1)-Tb(1)-O(5)	95.79(12)	O(4)-Tb(1)-O(6)	76.26(10)
O(3)-Tb(1)-O(5)	158.11(9)	O(5)-Tb(1)-O(6)	125.70(10)
O(4)-Tb(1)-O(5)	90.24(13)	O(2)-Tb(1)-O(6)	142.85(9)
O(1)-Tb(1)-O(2)	134.37(9)	O(7)-Tb(1)-O(6)	51.12(8)
O(3)-Tb(1)-O(2)	81.75(8)	O(1)-Tb(1)-N(1)	69.90(9)
O(4)-Tb(1)-O(2)	74.89(9)	O(3)-Tb(1)-N(1)	82.97(9)
O(5)-Tb(1)-O(2)	77.34(10)	O(4)-Tb(1)-N(1)	139.36(10)
O(1)-Tb(1)-O(7)	78.57(10)	O(5)-Tb(1)-N(1)	82.24(10)
O(3)-Tb(1)-O(7)	126.61(9)	O(2)-Tb(1)-N(1)	64.49(9)
O(4)-Tb(1)-O(7)	75.50(11)	O(7)-Tb(1)-N(1)	138.46(10)
O(5)-Tb(1)-O(7)	74.61(10)	O(6)-Tb(1)-N(1)	138.83(9)

Symmetry transformations used to generate equivalent atoms:

#1 -x+1/2,y+1/2,z #2 -x+1/2,y-1/2,z

Complex 2			
Dy(1)-O(1)	2.1781(19)	Dy(1)-O(2)	2.3665(18)
Dy(1)-O(3)	2.2340(18)	Dy(1)-O(6)	2.4850(19)
Dy(1)-O(4)	2.316(2)	Dy(1)-O(7)	2.4906(19)
Dy(1)-O(5)	2.344(2)	Dy(1)-N(1)	2.545(2)
O(1)-Dy(1)-O(3)	93.58(7)	O(2)-Dy(1)-O(6)	138.38(6)
O(1)-Dy(1)-O(4)	150.31(7)	O(1)-Dy(1)-O(7)	76.89(7)
O(3)-Dy(1)-O(4)	91.05(8)	O(3)-Dy(1)-O(7)	75.22(6)
O(1)-Dy(1)-O(5)	96.68(8)	O(4)-Dy(1)-O(7)	76.01(7)
O(3)-Dy(1)-O(5)	157.86(7)	O(5)-Dy(1)-O(7)	126.25(7)
O(4)-Dy(1)-O(5)	89.69(9)	O(2)-Dy(1)-O(7)	141.62(6)
O(1)-Dy(1)-O(2)	135.31(7)	O(6)-Dy(1)-O(7)	51.52(6)
O(3)-Dy(1)-O(2)	81.47(6)	O(1)-Dy(1)-N(1)	70.34(7)

O(4)-Dy(1)-O(2)	74.37(7)	O(3)-Dy(1)-N(1)	82.76(7)
O(5)-Dy(1)-O(2)	77.44(7)	O(4)-Dy(1)-N(1)	139.35(7)
O(1)-Dy(1)-O(6)	78.66(7)	O(5)-Dy(1)-N(1)	82.32(8)
O(3)-Dy(1)-O(6)	126.66(6)	O(2)-Dy(1)-N(1)	64.98(6)
O(4)-Dy(1)-O(6)	75.11(8)	O(6)-Dy(1)-N(1)	138.71(7)
O(5)-Dy(1)-O(6)	74.77(7)	O(7)-Dy(1)-N(1)	138.96(7)

Symmetry transformations used to generate equivalent atoms:

#1 -x+1/2,y-1/2,z #2 -x+1/2,y+1/2,z

Complex 3

Ho(1)-O(1)	2.175(3)	Ho(1)-O(2)	2.349(2)
Ho(1)-O(3)	2.216(2)	Ho(1)-O(6)	2.469(3)
Ho(1)-O(4)	2.307(3)	Ho(1)-O(7)	2.472(3)
Ho(1)-O(5)	2.326(3)	Ho(1)-N(1)	2.536(3)
O(1)-Ho(1)-O(3)	93.65(11)	O(2)-Ho(1)-O(6)	141.53(9)
O(1)-Ho(1)-O(4)	150.19(11)	O(1)-Ho(1)-O(7)	78.35(10)
O(3)-Ho(1)-O(4)	91.98(13)	O(3)-Ho(1)-O(7)	126.66(9)
O(1)-Ho(1)-O(5)	96.49(12)	O(4)-Ho(1)-O(7)	74.85(12)
O(3)-Ho(1)-O(5)	158.26(10)	O(5)-Ho(1)-O(7)	74.39(10)
O(4)-Ho(1)-O(5)	88.73(14)	O(2)-Ho(1)-O(7)	138.27(9)
O(1)-Ho(1)-O(2)	135.58(9)	O(6)-Ho(1)-O(7)	51.77(9)
O(3)-Ho(1)-O(2)	81.70(9)	O(1)-Ho(1)-N(1)	70.37(10)
O(4)-Ho(1)-O(2)	74.21(10)	O(3)-Ho(1)-N(1)	83.09(10)
O(5)-Ho(1)-O(2)	77.60(10)	O(4)-Ho(1)-N(1)	139.42(10)
O(1)-Ho(1)-O(6)	76.81(10)	O(5)-Ho(1)-N(1)	82.29(11)
O(3)-Ho(1)-O(6)	74.96(9)	O(2)-Ho(1)-N(1)	65.21(9)
O(4)-Ho(1)-O(6)	76.46(11)	O(6)-Ho(1)-N(1)	138.96(9)
O(5)-Ho(1)-O(6)	126.12(11)	O(7)-Ho(1)-N(1)	138.27(10)

Symmetry transformations used to generate equivalent atoms:

#1 -x+1/2,y+1/2,z #2 -x+1/2,y-1/2,z

Complex 4

Er(1)-O(1)	2.163(5)	Er(1)-O(2)	2.341(4)
Er(1)-O(3)	2.209(4)	Er(1)-O(7)	2.461(5)
Er(1)-O(5)	2.313(5)	Er(1)-O(6)	2.465(5)

Er(1)-O(4)	2.303(6)	Er(1)-N(1)	2.508(6)
O(1)-Er(1)-O(3)	93.97(19)	O(2)-Er(1)-O(7)	140.83(17)
O(1)-Er(1)-O(5)	96.7(2)	O(1)-Er(1)-O(6)	78.03(18)
O(3)-Er(1)-O(5)	158.50(18)	O(3)-Er(1)-O(6)	126.18(18)
O(1)-Er(1)-O(4)	149.59(19)	O(5)-Er(1)-O(6)	74.49(19)
O(3)-Er(1)-O(4)	92.8(2)	O(4)-Er(1)-O(6)	74.1(2)
O(5)-Er(1)-O(4)	87.4(3)	O(2)-Er(1)-O(6)	138.04(17)
O(1)-Er(1)-O(2)	136.48(17)	O(7)-Er(1)-O(6)	51.82(17)
O(3)-Er(1)-O(2)	81.69(17)	O(1)-Er(1)-N(1)	71.00(17)
O(5)-Er(1)-O(2)	77.72(18)	O(3)-Er(1)-N(1)	83.92(17)
O(4)-Er(1)-O(2)	73.86(18)	O(5)-Er(1)-N(1)	82.0(2)
O(1)-Er(1)-O(7)	76.63(18)	O(4)-Er(1)-N(1)	139.27(19)
O(3)-Er(1)-O(7)	74.45(16)	O(2)-Er(1)-N(1)	65.48(17)
O(5)-Er(1)-O(7)	126.24(19)	O(7)-Er(1)-N(1)	139.42(17)
O(4)-Er(1)-O(7)	76.8(2)	O(6)-Er(1)-N(1)	138.29(19)

Symmetry transformations used to generate equivalent atoms:

#1 -x+3/2,y+1/2,z #2 -x+3/2,y-1/2,z

Table S2 τ and v from the peak maxima of complex **2** at the corresponding temperatures from χ_M'' vs. v plots.

T (K)	$v_{\square \square \square}$ (Hz)	τ (s)
14.5	8066.776	1.97×10^{-5}
14	7418.225	2.15×10^{-5}
13.5	6418.004	2.48×10^{-5}
13	5519.503	2.88×10^{-5}
12.5	4682.74	3.4×10^{-5}
12	3949.117	4.03×10^{-5}
11.5	3296.097	4.83×10^{-5}
11	2722.074	5.85×10^{-5}
10.5	2219.729	7.17×10^{-5}
10	1784.843	8.92×10^{-5}
9.5	1415.794	1.12×10^{-4}
9	1105.096	1.44×10^{-4}
8.5	847.8129	1.88×10^{-4}
8	637.8227	2.5×10^{-4}

Table S3 The α parameters and τ of complex **2** from Cole-Cole analyses.

T (K)	α	τ (s)
6	0.078	1.03×10^{-3}
7	0.063	4.71×10^{-4}
8	0.054	2.46×10^{-4}
9	0.048	1.42×10^{-4}
10	0.043	8.80×10^{-5}
11	0.039	5.76×10^{-5}
12	0.037	3.95×10^{-5}
13	0.034	2.79×10^{-5}
14	0.036	1.98×10^{-5}
15	0.036	1.42×10^{-5}